

Accepted Manuscript

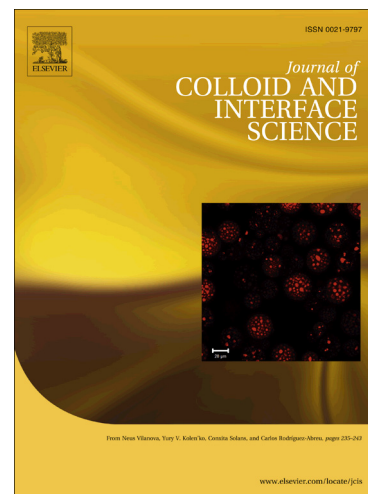
Advanced surface chemical analysis of continuously manufactured drug loaded composite pellets

Akter Hossain, Uttom Nandi, Ritesh Fule, Ali Nokhodchi, Mohammed Maniruzzaman

PII: S0021-9797(16)30895-5
DOI: <http://dx.doi.org/10.1016/j.jcis.2016.11.018>
Reference: YJCIS 21746

To appear in: *Journal of Colloid and Interface Science*

Received Date: 20 July 2016
Revised Date: 2 November 2016
Accepted Date: 6 November 2016



Please cite this article as: A. Hossain, U. Nandi, R. Fule, A. Nokhodchi, M. Maniruzzaman, Advanced surface chemical analysis of continuously manufactured drug loaded composite pellets, *Journal of Colloid and Interface Science* (2016), doi: <http://dx.doi.org/10.1016/j.jcis.2016.11.018>

This is a PDF file of an unedited manuscript that has been accepted for publication. As a service to our customers we are providing this early version of the manuscript. The manuscript will undergo copyediting, typesetting, and review of the resulting proof before it is published in its final form. Please note that during the production process errors may be discovered which could affect the content, and all legal disclaimers that apply to the journal pertain.

Advanced surface chemical analysis of continuously manufactured drug loaded composite pellets

Akter Hossain¹, Uttom Nandi¹, Ritesh Fule², Ali Nokhodchi^{3,4},
Mohammed Maniruzzaman^{3*}

¹Faculty of Engineering and Science, University of Greenwich, Central Avenue, Chatham Maritime, Chatham, Kent, ME4 4TB

²Faculty of Pharmaceutics Department, H.K. College of Pharmacy, Relief Road, Oshiwara, Jogeshwari West, Mumbai-400102, Maharashtra, India.

³Department of Pharmacy (Chemistry), School of Life Sciences, University of Sussex, Falmer, Brighton, UK BN1 9QJ

⁴Drug Applied Research Center and Faculty of Pharmacy, Tabriz University of Medical Sciences, Tabriz, Iran

***Correspondence:** M Maniruzzaman and Ali Nokhodchi, Email:
M.Maniruzzaman@sussex.ac.uk or M.Maniruzzaman12@gmail.com and
A.Nokhodchi@sussex.ac.uk; phone: +44(0)1273 877639.

ABSTRACT

The aim of the present study was to develop and characterise polymeric composite pellets by means of continuous melt extrusion techniques. Powder blends of a steroid hormone (SH) as a model drug and either ethyl cellulose (EC N10 and EC P7 grades) or hydroxypropyl methylcellulose (HPMC AS grade) as polymeric carrier were extruded using a Pharma 11 mm twin screw extruder in a continuous mode of operation to manufacture extruded composite pellets of 1 mm length. Molecular modelling study using commercial Gaussian 09 software outlined a possible drug-polymer interaction in the molecular level to develop solid dispersions of the drug in the pellets. Solid-state analysis conducted via a differential scanning calorimetry (DSC), hot stage microscopy (HSM) and X-ray powder diffraction (XRPD) analyses revealed the amorphous state of the drug in the polymer matrices. Surface analysis using SEM/energy dispersive X-ray (EDX) of the produced pellets arguably showed a homogenous distribution of the C and O atoms in the pellet matrices. Moreover, advanced chemical surface analysis conducted via atomic force microscopy (AFM) showed a homogenous phase system having the drug molecule dispersed onto the amorphous matrices while Raman mapping confirmed the homogenous single-phase drug distribution in the manufactured composite pellets. Such composite pellets are expected to deliver multidisciplinary applications in drug delivery and medical sciences by e.g. modifying drug solubility/dissolutions or stabilizing the unstable drug (e.g. hormone, protein) in the composite network.

Keywords: Amorphous, steroid hormone, ethyl cellulose, composite, continuous manufacturing, surface analysis.

1. Introduction

The term ‘continuous manufacturing’ in pharmaceutical sphere is referred to a process where pharmaceutical materials are produced in a continuous mode of operation with the scope of real time process monitoring [1]. In reality, the batch manufacturing that is the currently adopted manufacturing process, tests the products off-line after processing is complete lacking the opportunities of real time monitoring [1]. In contrary, the continuous manufacturing renders numerous benefits including those automated processing with less intermediate steps, flexible and cost effective operation. Besides, unlike the batch processing, continuous manufacturing also provides windows for on-line/in-line monitoring and product quality assurance for real time analysis [1-3].

Hot-melt extrusion (HME) has emerged and been employed as a novel manufacturing technique for the manufacture and development of various drug delivery systems over the last few decades [1]. Whilst, HME by itself is capable of integrating manufacturing process in a continuous mode of operation, a suitable exploitation of this emerging technique in pharmaceutical sphere has not yet been completely established [1]. The compatibility with a wider range of down streaming processing tools has HME one of most versatile manufacturing technology to produce pellets, granules, tablets, capsules and films with different therapeutic effects. These therapeutics effects can range from modified/controlled release through the mucosal or buccal delivery to medical implants and biodegradable composites [2, 5]. Though in the early eighty’s when HME was first introduced in pharmaceutical research, the initial research had primarily focused on the processing variables and instrumentations and their optimized use in the pharmaceutical drug delivery, more recent investigations have focused on the use of HME as a novel manufacturing technology to the development of medical implants, composite materials and nano-scale drug delivery systems [6,7]. Early studies via HME reported the manufacture of mini-tablets and the effect of the processing onto the sustained release of those drug loaded mini-tablets. The study reported that the manufactured mini-tablets contained ethyl cellulose and HPMC as polymeric carrier while poorly water soluble ibuprofen as a model drug [8, 9]. Similarly, vegetable calcium stearate (CaSt) was exploited as a suitable carrier to develop paracetamol loaded pellets to display a slow release of the drug [10]. Later studies showed the successful implementation of HME technique to manufacture and fabricate microbicide intravaginal ring (IVR) from polyether urethane (PU) elastomers. UC781 which is a nucleoside

reverse transcriptase inhibitor of HIV-1 was utilized as a model drug to treat AIDS [11]. These published reports so far have not only yielded many positive results but also many unanswered questions. For example: the detailed interpretation/description of the interactions between the drug and polymers used to develop solid dispersions/ dosage forms; the identity and validity of the manufactured products via a continuous platform and issues relating to the commercial scale-ups [1].

The optimisation and a combined formulation development strategy may prove efficient to develop novel composite materials [12-14] that controls the release of the drug and/or stabilise the physical state of the drug molecules in the composite matrices [15]. It has been reported that an optimized dosage form approach can overcome this problem to a certain extent; however, it requires a primeval manufacturing platform [16, 17]. It is therefore the purpose of this study to implement a continuous manufacturing HME processing to develop and characterize the composite pellets of a steroid hormone (SH) that can provide e.g. a sustained release of the drug for a prolonged period of time or overcome any associated physico-chemical (e.g. stability and compatibility) and technological (e.g. ease of operation, ease of scale up) issues. A formulation development strategy via continuous manufacturing of the novel SH composite pellets are hereby reported and the characterization of the drug polymer interactions and drug distribution in the composite pellets are studied.

2. Materials and method

2.1 Materials

Steroid hormone (SH) and PEG 2000 (PEG) were purchased from Sigma-Aldrich (Gillingham, Dorset, UK). Ethyl Cellulose N10 (EC N10), ethyl Cellulose EP7 (EC P7), HPMC AS-LF (HPMC) and compritol ATO-888 (C-888) were kindly donated by Hercules (Darmstadt, Germany), Colorcon Ltd. (Dartford, UK) and ShinEtsu (Japan) and Gattefosse (Toulouse, France), respectively. All solvents were bought from Fisher Chemicals (Loughborough, UK) and were of analytical grades.

2.2 Calculation of solubility parameters

Solubility parameters [18] were determined for the assessment of the possible miscibility of the drug with different polymers and were determined by utilizing the Hoftyzer and Van Krevelen method [19] as shown in the equation below:

$$\delta = \sqrt{\delta_d^2 + \delta_p^2 + \delta_h^2} \quad (1)$$

Here,

$$\delta_d = \frac{\sum F_{di}}{V_i}, \quad \delta_p = \frac{\sqrt{\sum F_{pi}^2}}{V_i}, \quad \delta_h = \sqrt{(\sum E_{hi} / V_i)}$$

i = structural groups within the molecule, δ = the total solubility parameter. F_{di} = molar attraction constant due to molar dispersion forces, F_{pi}^2 = molar attraction constant due to molar polarization forces, E_{hi} = hydrogen bonding energy, and V_i = molar volume.

2.3 Molecular Modelling

The dimeric structures of ethyl cellulose, HPMC and SH were computed by computational chemistry program Gaussview 09 [20]. The drug molecule was placed within the closeness of the dimeric structure of the polymer to outline the hydrogen bonding followed by the energy optimisation at the B3LYP 6-31G* level. The binding energy was calculated via a single point energies at the M06-2x/6-31G** level [16, 21]. The effect of basis set superposition error (BSSE) was corrected by employing counterpoise procedure.

2.4 Preparation of formulation blends and continuous HME processing

All SH formulations (as shown in Table 1) with EC N10, EC P7, HPMC/PEG and HPMC/C-888 were mixed in a Turbula TF2 mixer (Basel, Switzerland) in 100 g batches for 10 min each, prior to conducting the extrusion. Extrusion of all formulations were performed using a Pharma 11 twin-screw extruder (ThermoFisher, Germany) at 50°C/130°C/140°C-140°C/140°C/140°C (from feeding zone → Die) temperature profiles, 100 rpm screw speed. The extrudates (strands) produced were cut into pellets of 1 mm length using pelletizer (ThermoFisher, Germany).

2.5 Scanning electron microscopy (SEM)/ EDX analysis

SEM images of the flat cross-section of the pellets were captured using a cold-cathode field-emission gun scanning electron microscope (Hitachi SU8030 FEG-SEM, Japan) and Thermo-Noran (USA) EDX system with 30 mm² Ultra-Dry window and Noran 7 software. The

samples were glued with a double-sided carbon adhesive tabs and coated with carbon (Edwards 306 high vacuum carbon evaporation) prior to the SEM/EDX analysis. The accelerating voltage was set at 8 kV. Principal components were extracted from the X-ray maps using Noran 7 COMPASS software. The particle distribution on the surface area was characterized on the basis of chemical composition and morphology by using XPhase.

2.6 Atomic force microscopy (AFM)

An easyscan 2 (nanosurf, Switzerland) machine was used to take AFM photographs of the flat cross-sections of manufactured composite pellets on tapping mode by using tap 190Al-G cantilevers (BudgetSensors, Sofia, Bulgaria). The intermittent force between the oscillated tip and the substrate was kept to minimum by balancing the drive amplitude and the relative set point. SPIP software (Image Metrology, Hørsholm, Denmark) was utilised to analyse the images and for the data interpretations.

2.7 Thermal analysis

The solid state of the bulk drug, bulk polymers, mixtures of drug/polymers in different ratios and the pellets were studied by using a differential scanning calorimeter (DSC) 823e manufactured by Mettler-Toledo (Greifensee, Switzerland). Approximately, 3-5 mg of samples were weighed and taken in a sealed aluminium pans and heated at 10°C/min heating rates at the range of 25°C-250°C under an inert environment (nitrogen). The lids were pierced to allow the release of the excessive pressure generated upon heating.

The thermal analysis of the drug in the formulations was studied using a hot stage microscopy (Olympus BX60 microscope, Olympus Corp., USA) with Insight QE camera (Diagnostic Instruments, USA) was used to monitor the sample transitions. A FP82HT hot stage controlled by a FP 90 central processor (Mettler Toledo, Columbus, OH) was used to maintain temperatures between 20 and 250°C while a spot advance software (Diagnostic Instruments, Inc.) was utilised to capture the images.

2.8 Powder X-ray diffraction (XRPD)

The crystallinity of the SH in different composites was evaluated by using a Bruker D8 Advance (Germany) in theta-theta reflection mode with copper anode. For the purpose of the study pellets were ground to fine powders using a mortar and pestle prior to the analysis. A

parallel beam Goebel mirror with 0.2 mm exit slit and LynxEye sensitive detector opening at 3 degrees with 176 active channels was used. Each sample was scanned from 2 to 40 2θ with a step size of 0.02 2θ . Data collection and interpretations were performed using DiffracPlus and the EVA V.16 program, respectively.

2.9 Raman mapping

Raman spectra of bulk substances as well as the flat cross-section of the pellets were obtained at ambient using a Jobin/Yvon LabRam 320 instrument (1800 grooves/mm holographic grating, a holographic notch filter, a Peltier-cooled CCD (MPP1 chip) for detection) and an Olympus BX40 microscope equipped with an Olympus microscope (Horiba, Japan). An Ar⁺ ion laser ($\lambda = 532.8$ nm) was used. Raman spectra of the pellets were collected at ambient on a microscope slide using a microscope objective of 50 \times magnification to focus the laser beam. A backscattering (180° between excitation and collection) geometry was used in all experiments. Each spectral scan was collected for 5 s using 4 accumulations. The Raman instrument was calibrated using the ν_1 line of silicon at 520.7 cm^{-1} . Using the frequencies of the principal lines of a neon lamp checked centering of the silicon line. The experimental conditions for Raman mapping of the pellets were: 100 nm slit width, a 50 \times Microsoft objective and 0.4 s acquisition time. Each spectrum was the mean of the two. The sample profiling was performed at step increments of 3 μm in the X–Y direction covering the biggest possible surface of the part.

3. Results and discussion

3.1 Solubility parameters and molecular modelling

The drug/polymer miscibility was estimated by correlating the energy of mixing from inter and intra-molecular interactions of the materials used (drug and polymers) [19]. For this purpose, the Hansen parameters (δ) calculated based on the structural orientation of the component informs that the drug-polymers with similar δ values used in a system are likely to interact with each other as matter of being miscible. It has widely been accepted that two compounds are generally treated miscible when $\Delta\delta$ is less than 7 $\text{MPa}^{1/2}$ (17, 20) [19]. The higher values of $\Delta\delta$ (>7 $\text{MPa}^{1/2}$) between a drug/polymer pair generally indicates an immiscibility. In general term, the miscibility is achieved by balancing the energy of mixing released by inter-molecular interactions with that of intra-molecular interactions within the components [22, 23]. In this study, the calculated solubility parameters of SH, EC N10, EC P7

and HPMC are 22.60, 25.61, 25.27 and 25.30 MPa^{1/2}, respectively. The difference between the calculated solubility parameters of each drug/polymer pair indicates that SH is likely to be miscible with all polymers. The $\Delta\delta$ values reported for SH/EC N10, SH/EC P7 and SH/HPMC are 3.01, 2.67 and 2.70 MPa^{1/2}, respectively. As a result, based on the theoretical calculations, the miscible systems should result in the formation of molecular solid dispersions. Similar claims have been made previously in various literature [22, 23]. In order to interrelate the theoretical calculations to that of experimental findings, the solid state thermal analysis (see DSC section for more details) should reveal a single glass transition (T_g) at an intermediate temperature between the T_g s of the amorphous polymer and the amorphous drug, if a molecular dispersion is formed. Moreover, due to the strong miscibility as determined herein by the solubility parameters, the drug molecules are expected to have been entrapped in the composite matrices to form solid dispersions at a molecular level. This has been validated by solid state analyses below. As a matter of fact, all manufactured composite pellets showed a homogenous drug dispersion throughout the manufactured pellets (see surface analysis sections).

Quantum mechanical (QM)-based molecular modelling approach was utilised to compute the binding energy between the drug and the polymers by considering total energy of the system in all possible atomic co-ordinations. Any non-bonded interactions such as hydrogen bonds can be calculated precisely via the QM approach adopted in this study. The calculated binding energy represents the strengths of the hydrogen bonds between the drug and polymers (Fig. 1). The calculated binding energy indicated that the interactions and thus the possible miscibility between the drug molecule and the polymers are quite high ranging from 15-25 kcal/mol resemblance of the numbers of H-bonds. Similar to the solubility parameters calculations, it can be claimed via the QM approach that the higher the binding energy the more stable the drug/polymer interactions to develop the solid dispersions in the composites [16].

3.2 Manufacturing of composite pellets

Extrusion processing optimised to obtain the extrudates as white composite pellets of 1 mm length is depicted in Fig. 2. The temperature profiles, screw speed and the feed rate were found to be the critical processing parameters (CPP) for the development of the composite pellets. During the optimisation of the process to manufacture composite pellets, a range of temperatures profiles from 120°C-140°C were evaluated to assess the final outputs such as shear force, torque, feed rate and screw speed on the manufactured pellets. The optimised screw configuration provided intermediate levels of distributive mixing. This is typical of the type of

screw configurations used in conventional polymer compounding (mixing) operations. Distributive mixing was achieved and optimised in the process during extrusion using a series of bi-lobal mixing/ kneading blocks or paddles. These blocks are of length equal to a quarter of the extruder screw diameter and were arranged at specified angles from the preceding element: 30, 60 or 90° in the forward conveying direction. It is noted that a kneading block arrangement with a 30° mixing paddles provide the most forward conveying while 60° provide moderate to less and 90° provide complete mixing with zero forward conveying action.

By keeping the final processing condition and the throughput of the drug/polymer/plasticizers powder blends, final batch of formulations extruded continuously at 140°C with a feed rate of 1 kg/h and a high screw speed of 100 rpm produced polymeric strands with uniform shape and of about 1 mm diameter. The pellets obtained via an automated pelletizer consistently produced pellets of 1 mm length.

3.3 SEM and EDX analysis

SEM examined surface morphology for both the drug and extruded composite pellets. The extrudates containing both polymers exhibited no drug crystals on the extrudate surface with SH (Fig. 3a). A homogenous particle distribution was observed on the surface of manufactured pellets. SEM-EDX was performed to determine the distribution of SH in the continuously manufactured composite pellets. Both of the polymeric carriers used mainly contain C and O atoms, similar to the drug. The distribution of SH was visualized by EDX elemental mapping of C and O only (Fig. 3b). The most occupied element was carbon (C) as it is the most abundant element comprising a majority of APIs and additives for oral drug delivery including SH and polymers used in this study. In this study, most of the phases showed a similar set of atomic textures due to the homogeneous distribution of the combined substances. Therefore, it was quite difficult to identify any specific phase in the absence of any marker atoms of the drug SH. However, this result provided evidence that the pellets were well formed in the intended drug-polymer ratio without the occurrence of irregular content strain during the continuous production of pellets via HME processing. This irregular content strain could have been evident due to the presence of inhomogeneous drug/excipients distribution in the composite materials. It was also evaluated that the SH was homogeneously dispersed into the particle matrix by EDX mapping

study. Recently, there have been some reports about EDX mapping used for the observation of homogenous distribution of API on extruded formulations [17].

3.4 Atomic force microscopy (AFM)

AFM was applied, as a complementary technique [24] to investigate whether SH was dispersed/entrapped in matrices of the polymers/plasticizers (for F3 and F4) [25]. The AFM images of the composite pellets are illustrated in Fig. 4. The phase images in Fig. 4 showed that there is no phase separation between the components indicating that SH has been adsorbed by the carriers during the extrusion processing. Moreover, there was no sign of crystallisation on the surface, which also indicates the presence of the drug in amorphous state within the matrices. Fig. 4 also indicates that a homogenous mixing was performed during the continuous HME processing which could be due to the possible intermolecular interactions as outlined via the molecular modelling studies. The topographic AFM image demonstrates the roughness of the surface which is also presented in the SEM results. Surface roughness were identified in the root mean square (RMS) value and has been estimated to be 132.26 (± 62) nm. This roughness can be due to the manufacturing procedure. The observed results were consistent with all drug/polymer ratios with or without plasticizer for extruded formulations suggesting that even at high drug loading HME processing resulted in a homogenous single phase solid dispersions.

3.5 Thermal analysis

The thermal transitions of the bulk drug, polymers and the formulations were analysed by DSC. The overall findings from DSC results are summarized in Fig. 5a and b. The DSC scan of bulk SH in Fig. 5a showed an endothermic sharp transition due to its melting at 226.12 °C ($\Delta H = 114.92$ J/g). The bulk polymers showed thermal events (step change) at 133.01 °C, 117.61 °C and 128.21 °C conforming to the T_{gs} of EC N10, EC P7 and HPMC, respectively (Fig. 5a). Similar to the bulk drug, both crystalline PEG and C-888 showed thermal events at 52.82 °C and 72.14 °C, respectively due to their meltings. All drug polymer physical blends showed endothermic transitions (Fig. 5b) due to the presence of the initial crystalline substances at slightly shifted positions. These crystalline melting peaks were not visible in all extruded composite pellets. The extruded formulations exhibited only one broad endothermic peak in the region of 47.83 to 49.19 °C indicating the presence of the drug in the molecular dispersion state. Being trailed by the statement made in the solubility parameter section above, it is claimed that the

intermediate position of the single endotherm in the extruded formulations between the T_g s of amorphous drug and the polymers indicates the formation of molecular solid dispersion [22, 23]. Also, according to Gordon Taylor equation in a miscible drug/polymer system a broad single T_g would appear at an intermediate position of the T_{gs} of amorphous drug and the polymer [23].

Thermal analysis conducted via HSM determined the thermal transitions due to the melting of crystalline SH within the polymer matrices as a function of heating. Various images of both the bulk drug and drug/polymer mixtures taken using HSM are depicted Fig. 5c. Bulk SH showed minimal thermal change upon heating up until 200-220°C (data not shown), complemented by the DSC findings (melting at 226°C). All composite extruded pellets showed complementary thermal events similar to the DSC analysis for an example, SH in ethyl cellulose matrices showed nominal API melting until reaching temperatures of 195-202°C followed by extensive/complete melting of the drug (Fig. 5c). Likewise, the drug/EC P7 system showed the extensive melting of the drug within the polymer matrix at slightly low temperature at 185°C. Similar complementing results were obtained for HPMC systems in the presence of PEG and C-888.

3.6 X-ray powder diffraction (XRD) analysis

X-ray powder diffraction analysis was utilised to examine the API crystalline state. As depicted in Fig. 6 the diffractograms of pure SH presented distinct crystalline peaks at 5.75, 14.50, 16.08, 17.42, 18.79, 19.42, 23.22, 29.21, 30.14 2 θ .

The physical mixture of all formulations presented identical peaks of the crystalline substances present in the system but at lower intensities suggesting that the drug retained its crystalline properties. No such crystalline distinct peaks were found any of the extruded formulations in ethyl cellulose polymeric systems. Similarly, no distinct intensity peaks corresponding to SH was observed in the diffractograms of the extruded formulations in the HPMC systems except for the low intense peak due to the presence of crystalline PEG/C-888 in the formulations. The absence of SH intensity peaks in the extruded formulations simply indicates the presence of amorphous API.

3.7 Raman mapping

Raman spectra and the mapping of the surface [26-29] of the composite pellets are depicted in Fig. 7 and 8. As it can be observed, SH has a characteristic peak at $1600\text{-}1700\text{ cm}^{-1}$, which has been used to investigate the distribution of the drug in the formulations by means of univariate analysis. Fig. 7 and 8 demonstrate the consistent and homogeneous distribution of SH in all the particle area in physical mixtures (red dot represents SH, green dot represents HPMC polymer and blue dots represents PEG/C-888) of F3 and F4, respectively. Also it shows that all other materials are homogeneously mixed in the formulation. In contrast, the extruded composite pellets demonstrates a homogeneous one phase system represented by a full green view which may indicate the presence of HPMC polymer and drug encapsulated within the polymer matrices as claimed by DSC and XRPD analysis above (F3). Similarly, the surface mapping of F4 (Fig. 8) shows a very different blue/dark background corresponding to the polymer. The existence of the single phase homogenous system in all formulations indicates that the drug molecule has been encapsulated within the polymeric matrices. This could also happen due to the molecular interaction as a result of single-phase distribution [30].

Histograms of all formulations (Fig. 7 and 8) showed that the major components of the formulations were identical in composition. A change in peak is observed because of the third component (PEG/C-888) of each formulations.

4. Conclusions

In the current study HME was successfully utilised as a robust continuous manufacturing platform to develop SH loaded composite pellets. Molecular modelling simulation used as a predictive tool to estimate the possible drug-polymer miscibility/interactions to develop composites showed a strong binding energy between the drug and polymer. This high interaction energy may play a pivotal role to develop the composite pellets having the drug molecularly dispersed in the system. The solid-state analysis revealed the existence of the drug in molecular dispersion state during the processing while advanced surface analysis showed a homogenous single-phase. Such emerging approach can be utilised to develop controlled release drug delivery systems. Moreover, the development of the SH based composite pellets via HME is preferable since its preparation is quick, economical with fewer process steps which will make the future pilot scale formulation development much easier.

Declaration of interest: The authors report no declarations of interest.

References

1. M. Maniruzzaman, D. Douroumis, *Int. J. Pharm.* 496(1) (2015) 1-2.
2. M.A. Repka, S.K. Battu, S.B. Upadhye, S. Thumma, M.M. Crowley, F. Zhang, C. Martin, J.W. McGinity, *Drug Dev. Ind. Pharm.* 33 (2007) 1043–1057.
3. M. Maniruzzaman, A. Nair, N. Scoutaris, M.S. Bradley, M. J. Snowden, D. Douroumis, *Int. J Pharm.* 496(1) (2015) 42-5.
4. F. Zhang, J.W. McGinity, *Pharm. Dev. Tech.* 4(2) (1999) 241–250.
5. M. Maniruzzaman, A. Nair, M. Renault, U. Nandi, N. Scoutaris, R. Farnish, M.S. Bradley, M.J. Snowden, D. Douroumis, *Int. J Pharm.* 496(1) (2015) 52-62.
6. K.T. Campbell, D.Q.M. Craig, T. McNally, *J. App. Pol. Sci.* 131(10) (2014) 40284-91.
7. K.T. Campbell, S. Qi, D.Q.M. Craig, T. McNally, *J. Pharm.Sci.* 98 (2009) 4831.
8. C. De Brabander, C. Vervaet, L. Fiermans, J.P. Remon *Int. J. Pharm.* 199 (2000) 195-203.
9. C. De Brabander, C. Vervaet, J.P. Remon, *J. Cont. Rel.* 89 (2003) 235–247.
10. E. Roblegg, E. Jäger, A. Hodzic, G. Koscher, S. Mohr, A. Zimmer, J. Khinast, *Eur. J. Pharm. Biopharm.* 79 (2011) 635–645.
11. M.R. Clark, T.J. Johnson, R.T. McCabe, J.T. Clark, A. Tuitupou, H. Elgendy, D.R. Friend, P.F. Kiser, *J Pharm. Sci.* 101(2) (2012) 576-87.
12. F. Kuralay and A. Erdem, *Analyst*, 140 (2015) 2876-2880.
13. Y. Wen, M.R. Gallego, L. F. Nielsen, L. Jorgensen, E.H. Møller, H. M. Nielsen, *Eur. J Pharm. Biopharm.* 85(1) (2013) 87-98.
14. H. Sato, M. Fujimori, H. Suzuki, K. Kadota, Y. Shirakawa, S. Onoue, Y. Tozuka, *Eur. J Pharm. Bopharm.* 92(2015) 49-55.
15. K.T. Campbell, D.Q.M. Craig, T. McNally, *Int. J. Pharm.* 363 (2008) 126.
16. M. Maniruzzaman, J. Pang, D. J. Morgan and D. Douroumis, *Mol. Pharm.* 12(4) (2015) 1040–1049.
17. K. Vithani, M. Maniruzzaman, I. J. Slipper, S. Mostafa, C. Miolane, Y. Cuppok, D, *Colloids Surf. B.* 110 (2013) 403–410.
18. C. M. Hansen, *Ind. Eng. Chem. Prod. Res. Dev.* 8 (1969) 2–11.
19. D. J. Greenhalgh, W. Peter, T.P. York, *J Pharm Sci.* 1999; 88: 1182–1190. *J. Pharm. Sci.* 88 (1999) 1182–1190.

20. R. Dennington, T. Keith and J. Millam, Gauss View, Version 5, Semichem Inc., Shawnee Mission KS, 2009.
21. Y. Zhao and D. G. Truhlar, Theor. Chem. Acc. 120 (2008) 215–241.
22. M. Maniruzzaman, M.M. Rana, J.S. Boateng, J.C. Mitchell, D. Douroumis, Drug Dev. Ind. Pharm. 39(2) (2013) 218-27.
23. X. Zheng, R. Yang, X. Tang and L. Zheng, Drug Dev. Ind. Pharm. 33 (2007) 791–802.
24. X. Hu and C. Z. Dinu, Analyst, 140 (2015) 8118-8126.
25. H.S. Purohit, L.S. Taylor, Mol. Pharm. 12(12) (2015) 4542-53.
26. J. Cyriac, M. Wleklinski, G. Li, L. Gao and R. G. Cook, Analyst, 137 (2012) 1363-1369.
27. G. Verstraete, J. Van Renterghem, P.J. Van Bockstal, S. Kasmi, B.G. De Geest, T. De Beer, J.P. Remon, C. Vervaet, Int. J. Pharm. 506(1-2) (2016) 214-221.
28. B.A. Palmer, A. Le Comte, K.D. Harris, F. Guillaume, J. Am. Chem. Soc. 135(39) (2013) 14512-5.
29. K. Punčochová, B. Vukosavljevic, J. Hanuš, J. Beránek, M. Windbergs, F. Štěpánek, Eur. J. Pharm. Biopharm. 101 (2016) 119-125.
30. M. T. Islam, N. Scoutaris, M. Maniruzzaman, H. G. Moradiya, S. A. Halsey, M. S.A. Bradley, B. Z. Chowdhry, M. J. Snowden, D. Douroumis, Eur. J. Pharm. Biopharm. 96 (2015) 106-116.

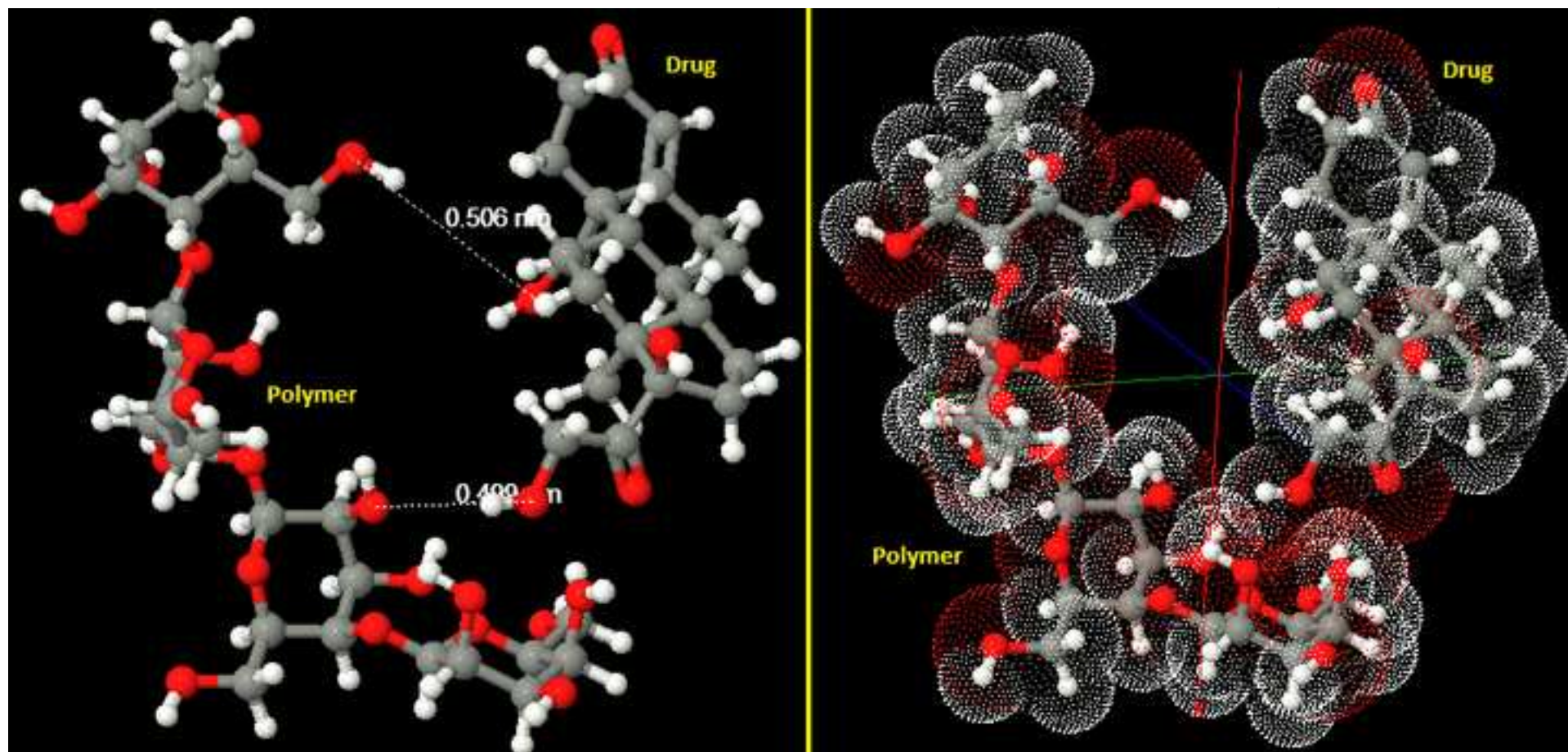
TABLE(S)

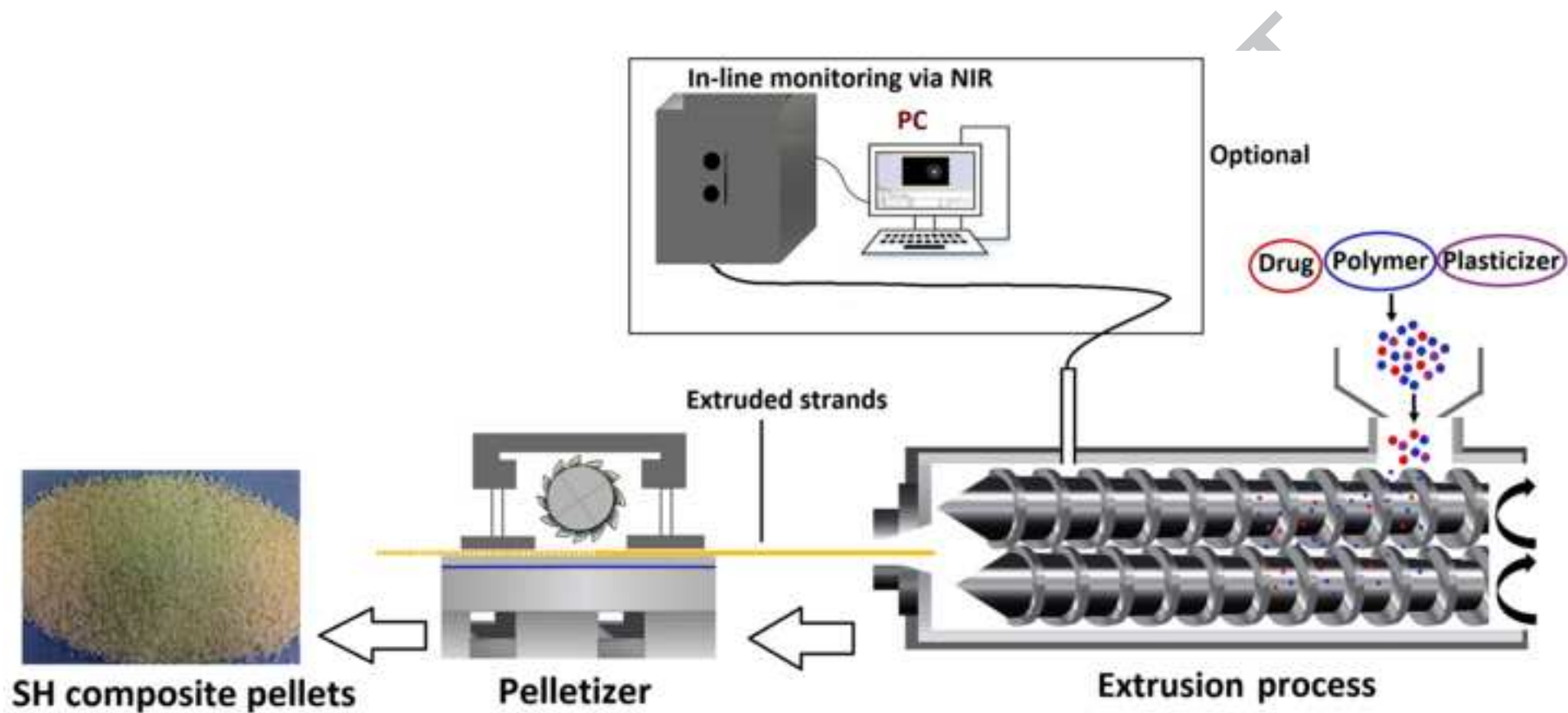
Table 1: Formulation composition of the SH composite pellets

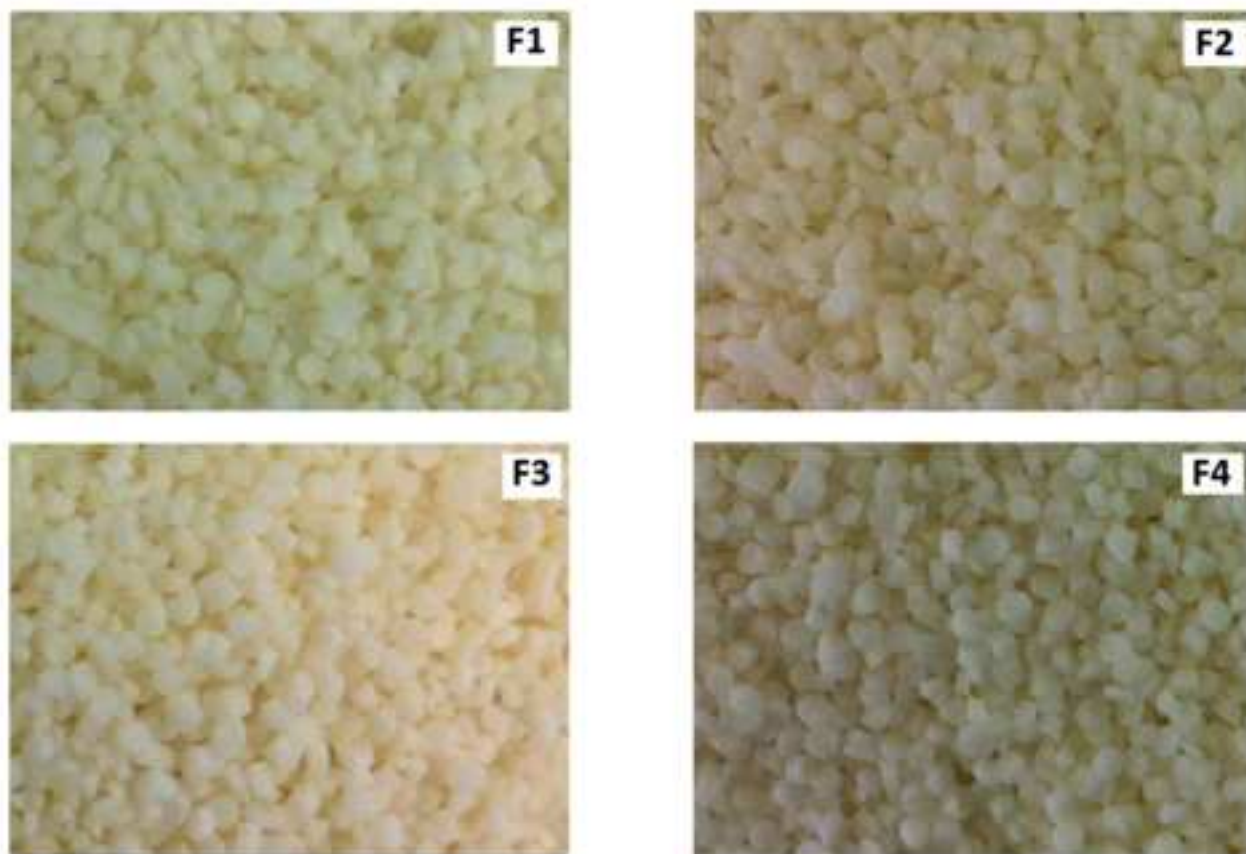
Formulation	SH (%)	EC N10 (%)	EC P7 (%)	HPMC (%)	PEG (%)	ATO-888 (%)
F1	30	70				
F2	30		70			
F3	30			60	10	
F4	30			60		10
F5	40	60				
F6	40		60			

Figures caption list

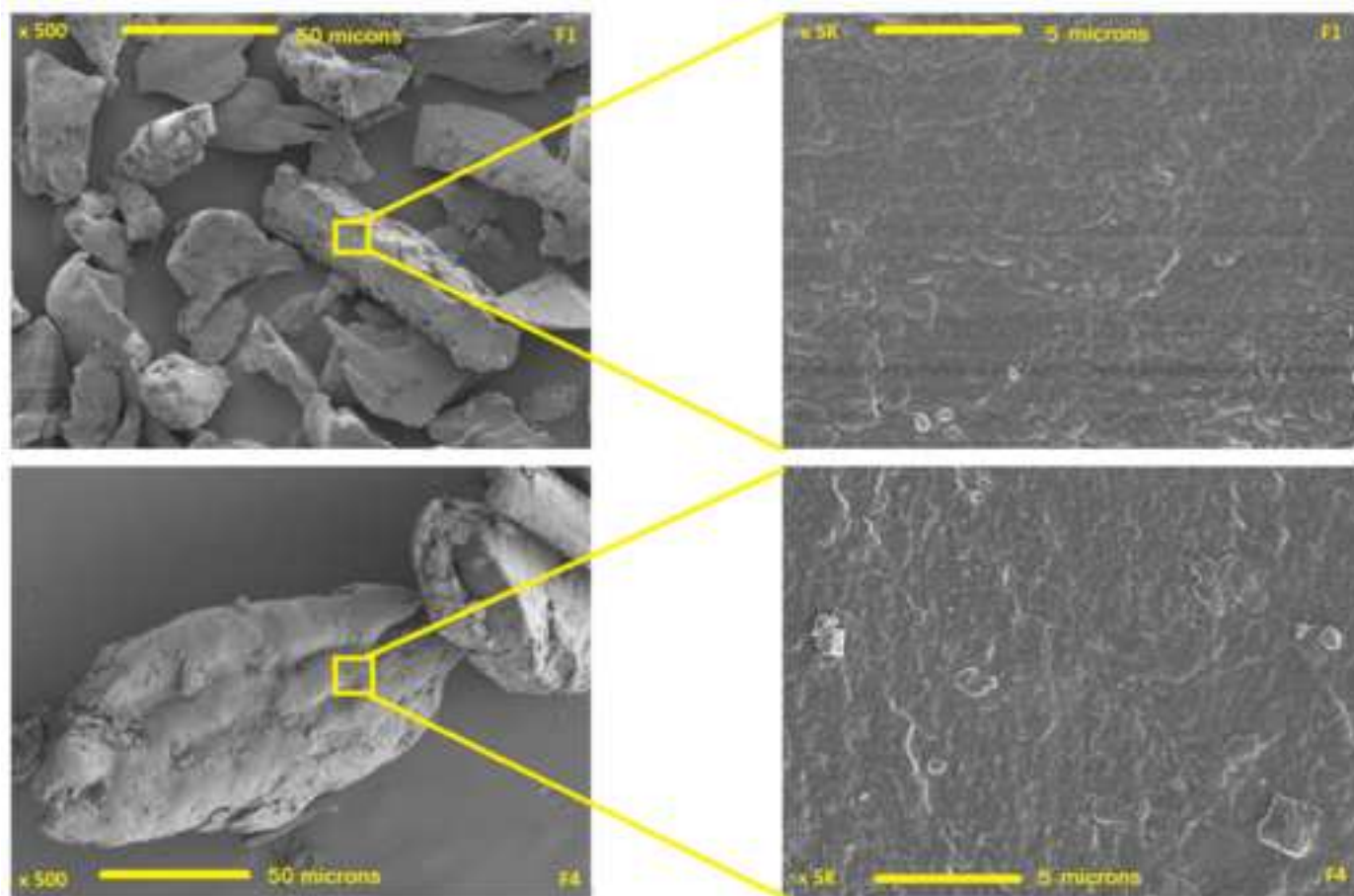
Fig. 1	Molecular modelling to predict drug/polymer intermolecular interaction.
Fig. 2	Continuous manufacturing process of SH pellets using HME.
Fig. 3a	Optical images of pellets and SEM images of the pellets of SH/polymers.
Fig. 3b	EDS surface analysis of the pellets.
Fig. 4	AFM images of the composite pellets; (a) phase and (b) topographic images of extruded composite pellets.
Fig. 5a	DSC thermal analysis of pure drug and polymers.
Fig. 5b	DSC thermal transition of the physical blends and extruded pellets.
Fig. 5c	HSM images to show the thermal transition of SH in the polymeric matrices.
Fig. 6	XRPD diffractograms of pure drug, drug/polymer physical mixtures (PM) and extruded formulations (EXT).
Fig. 7	Raman mapping and spectra of (a) physical mixture and (b) the composite pellets (F3).
Fig. 8	Raman mapping and spectra of (a) physical mixture and (b) the composite pellets (F4).



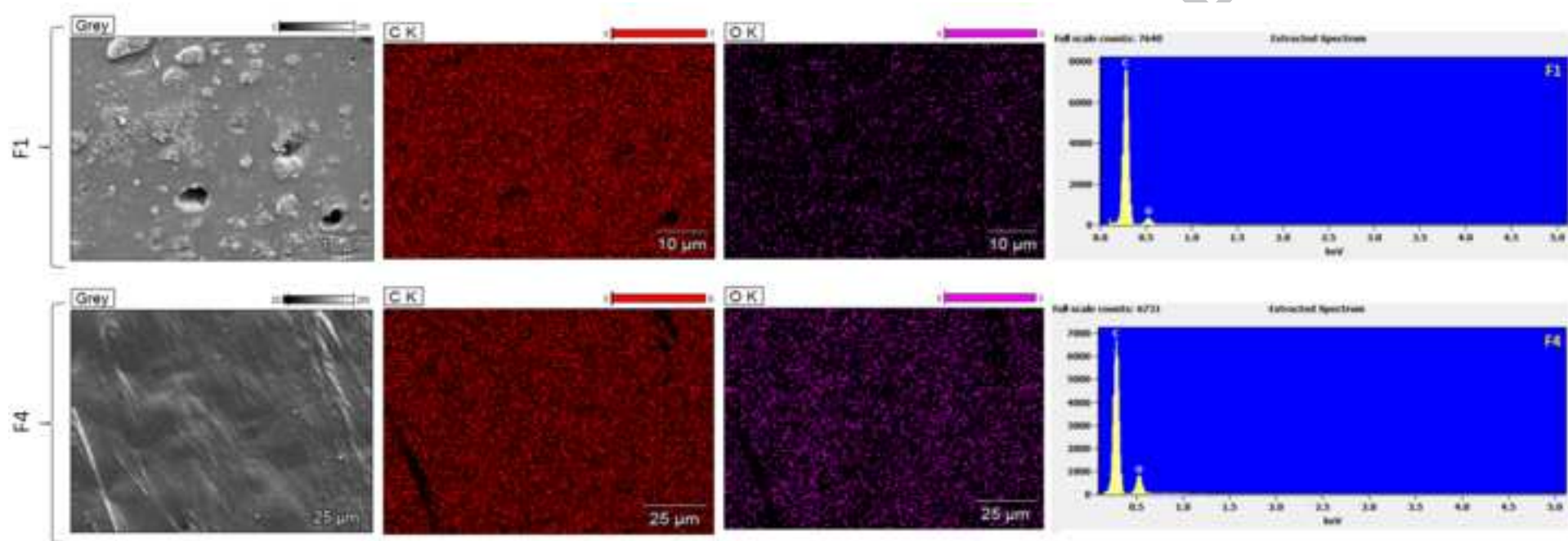




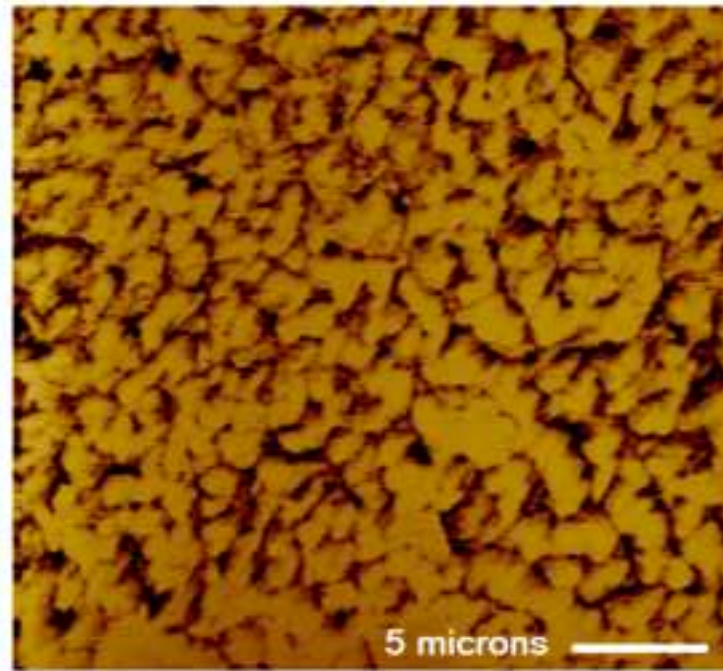
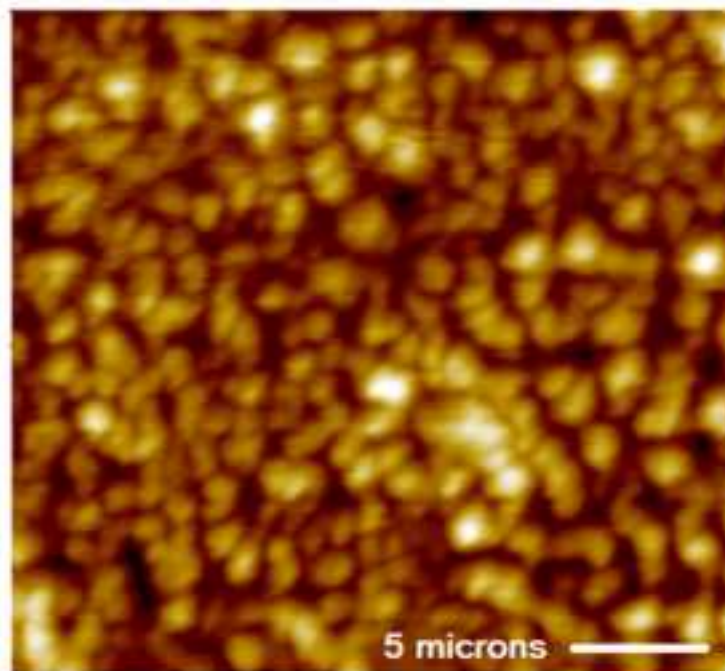
(a)



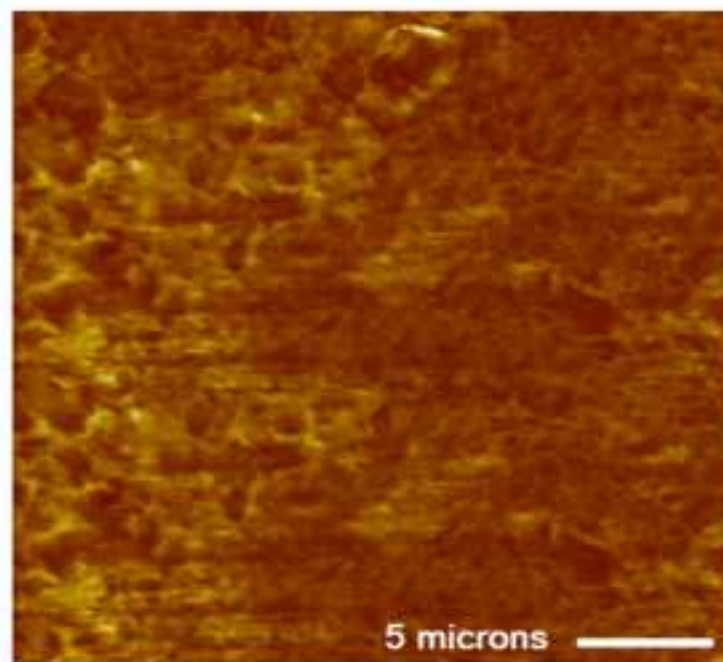
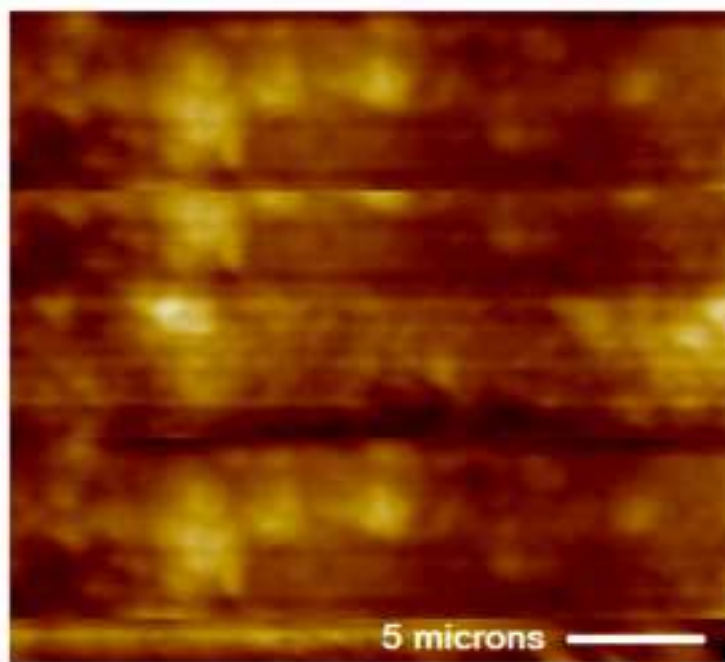
(b)



F3

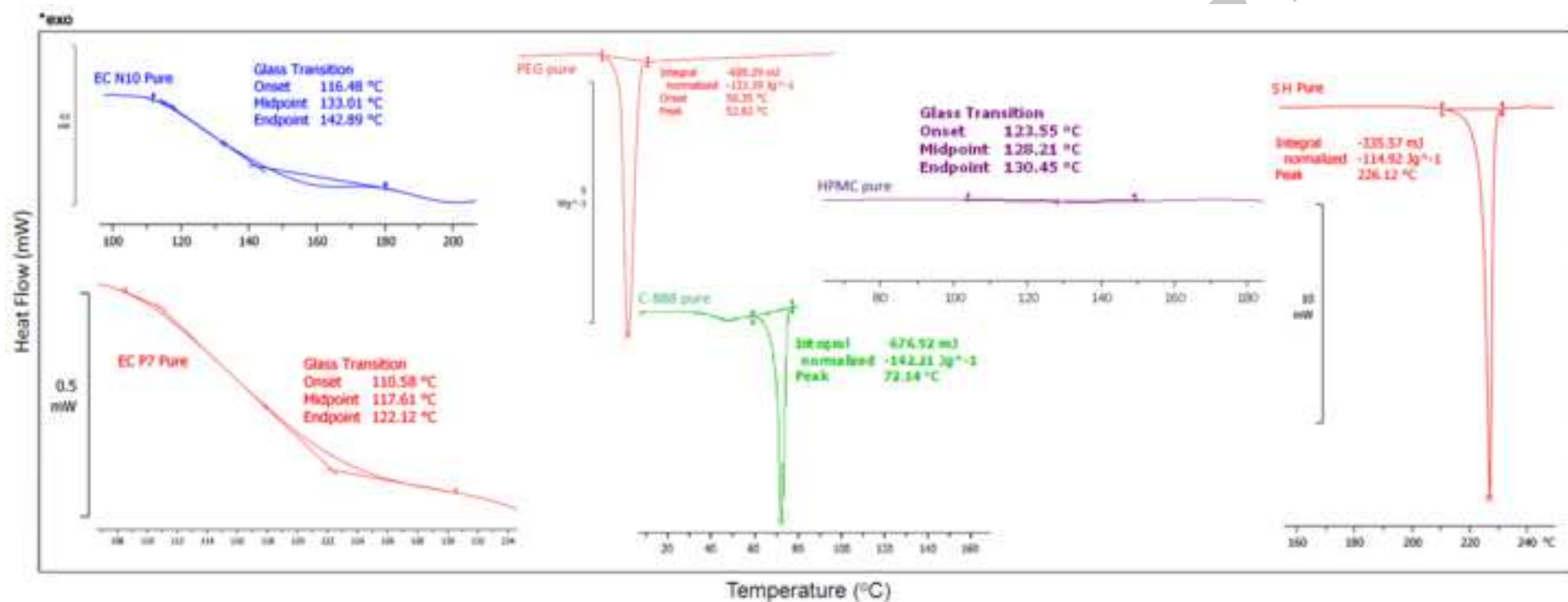


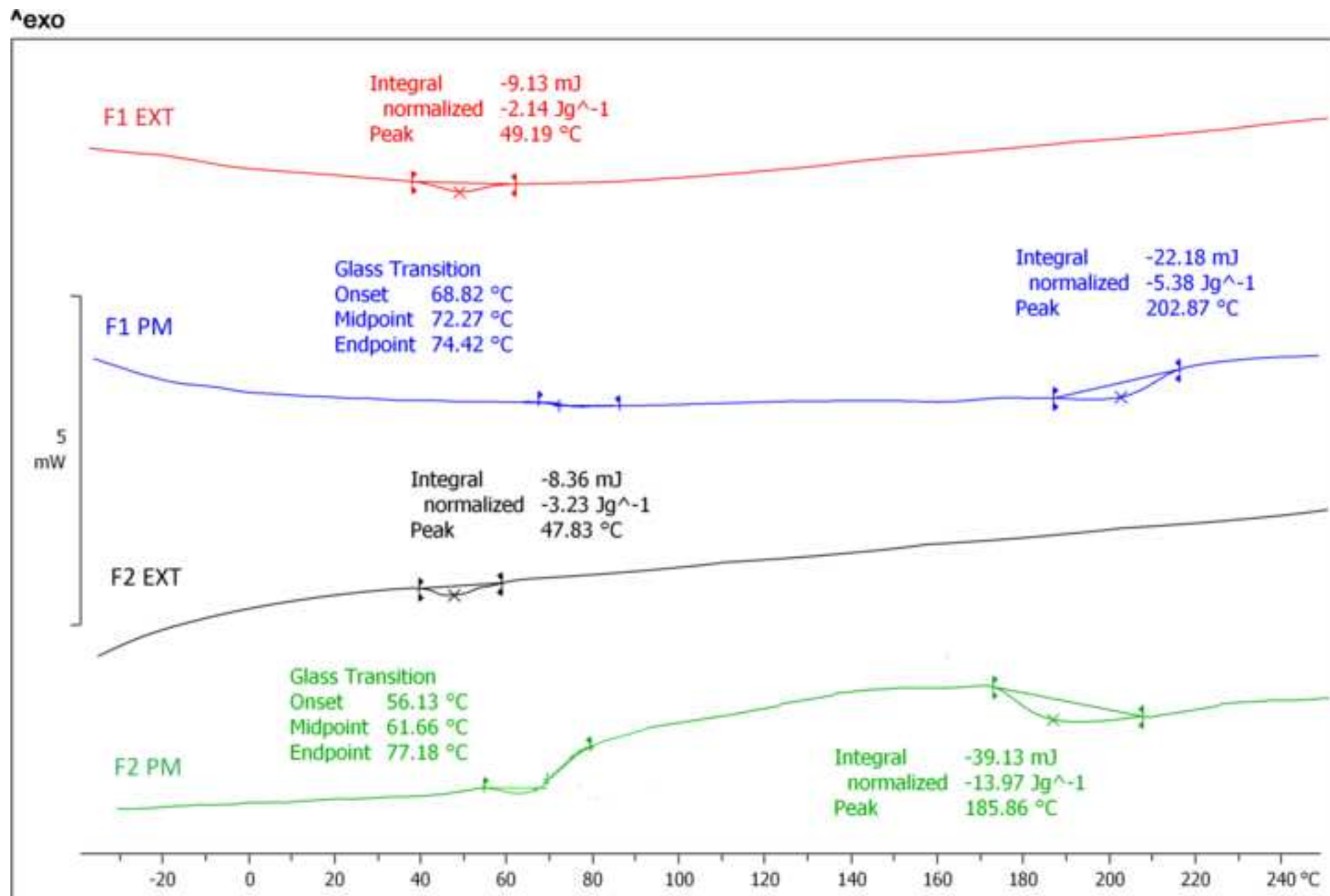
F4

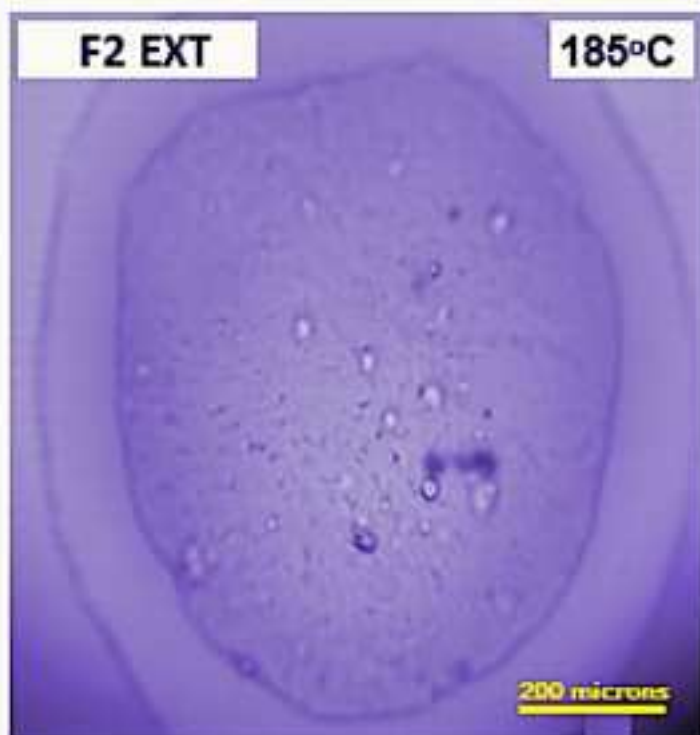
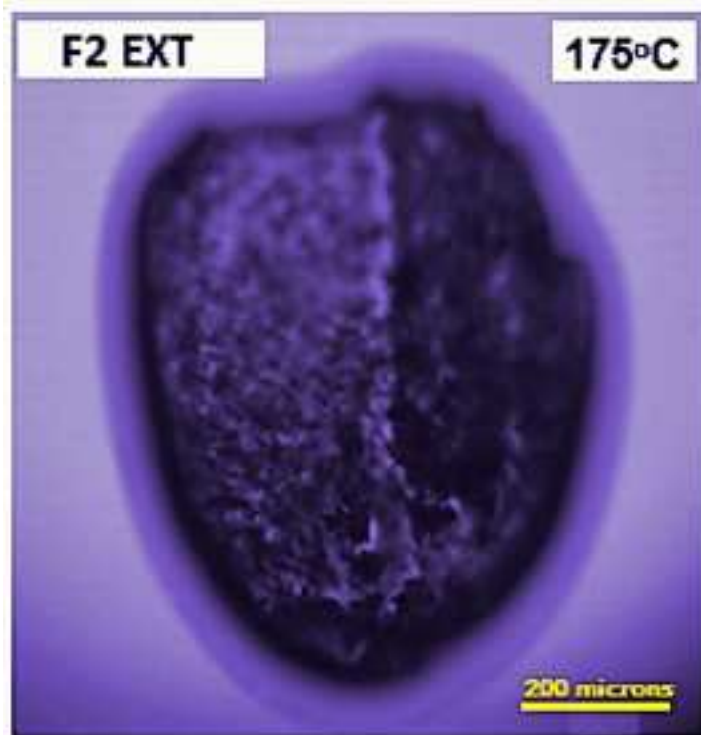
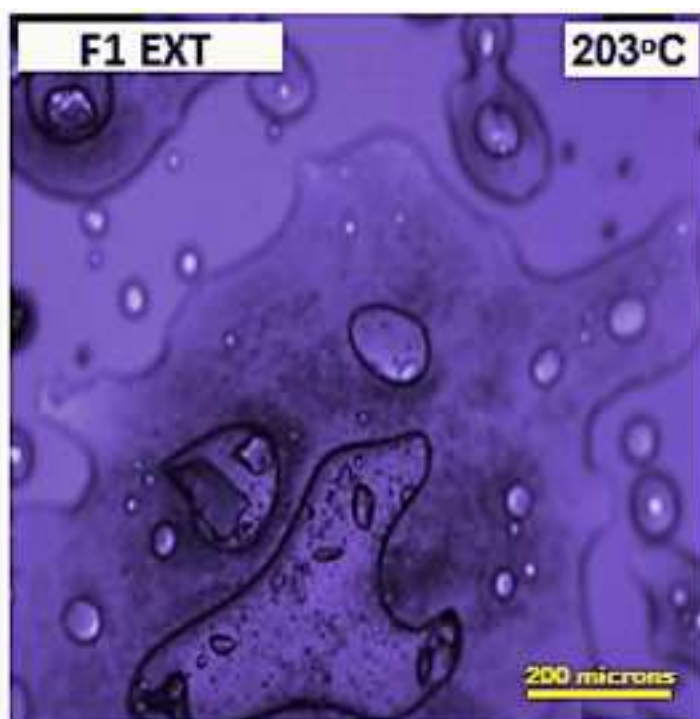
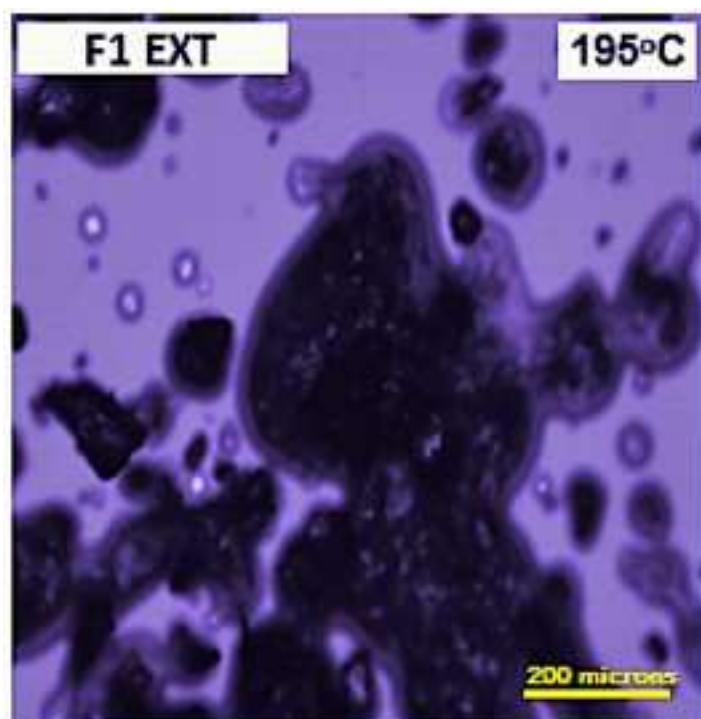


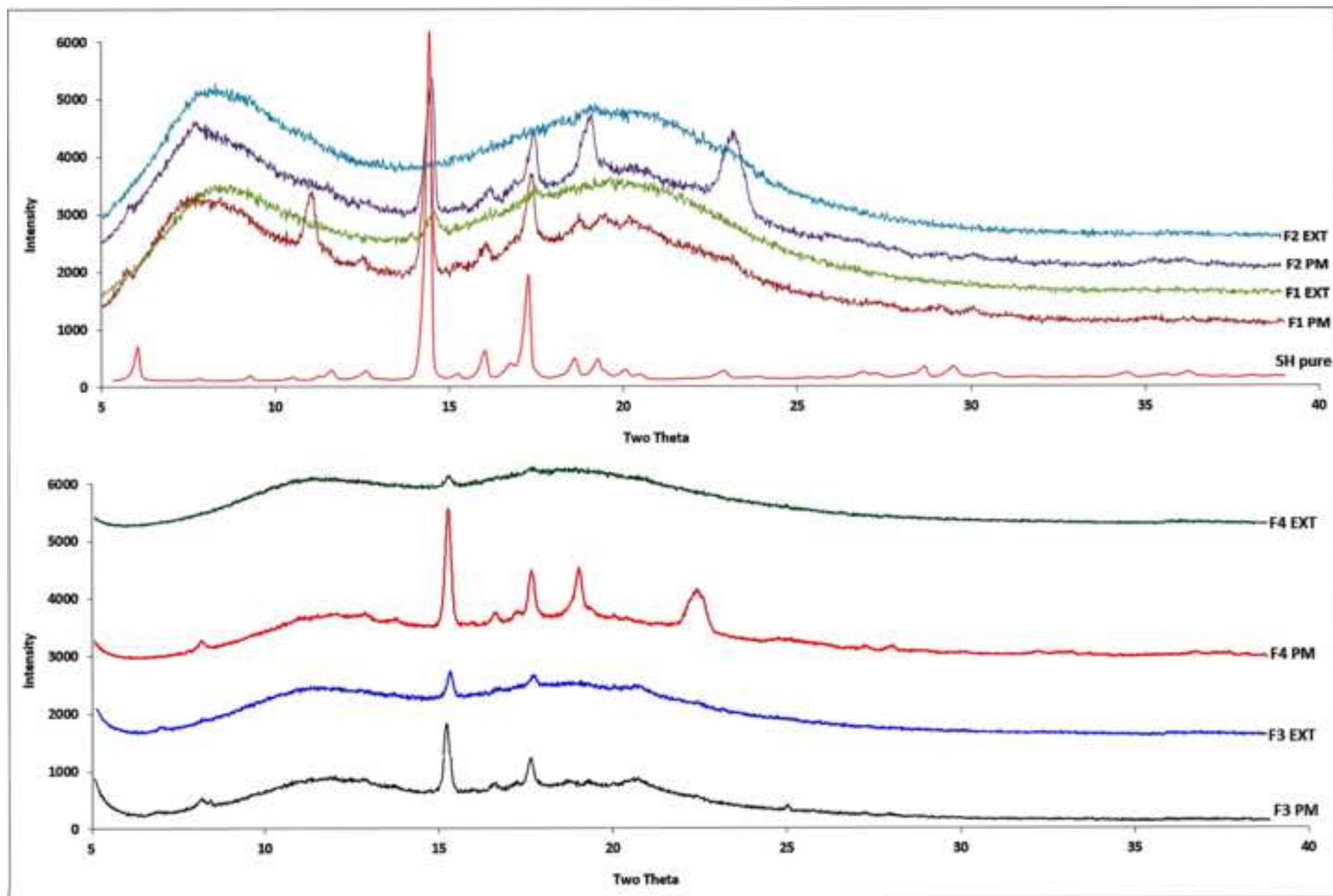
(a)

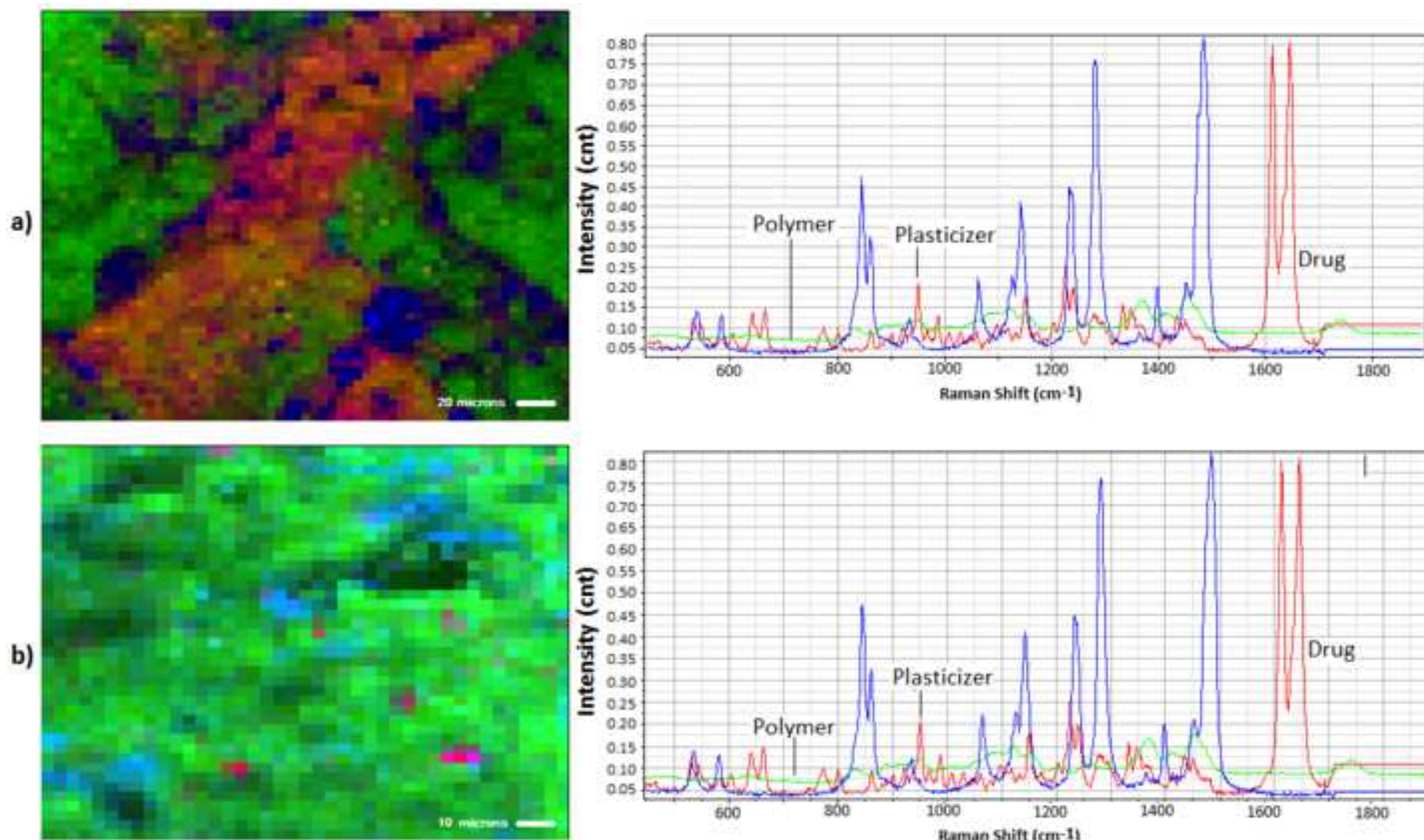
(b)



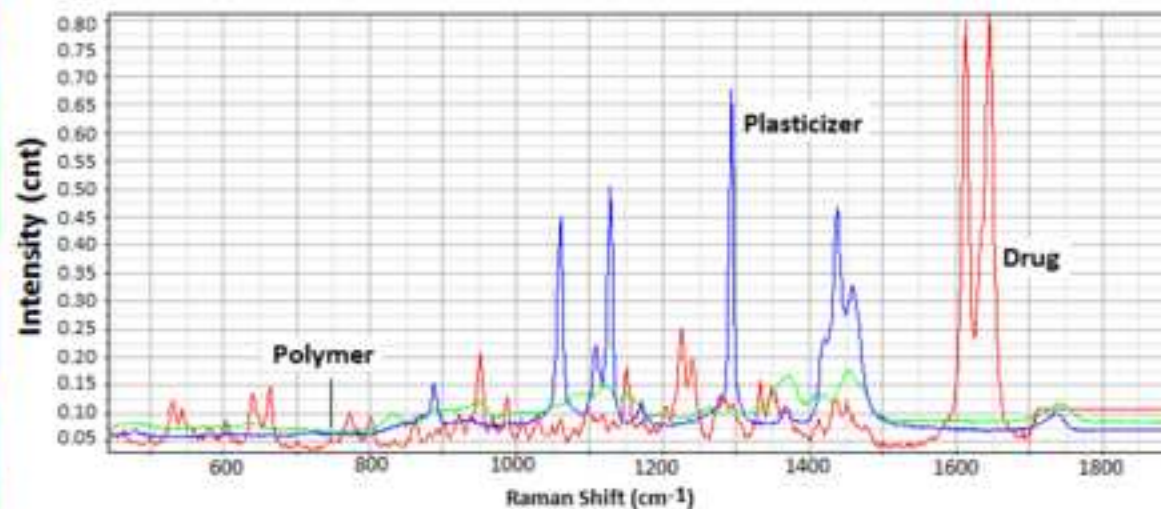
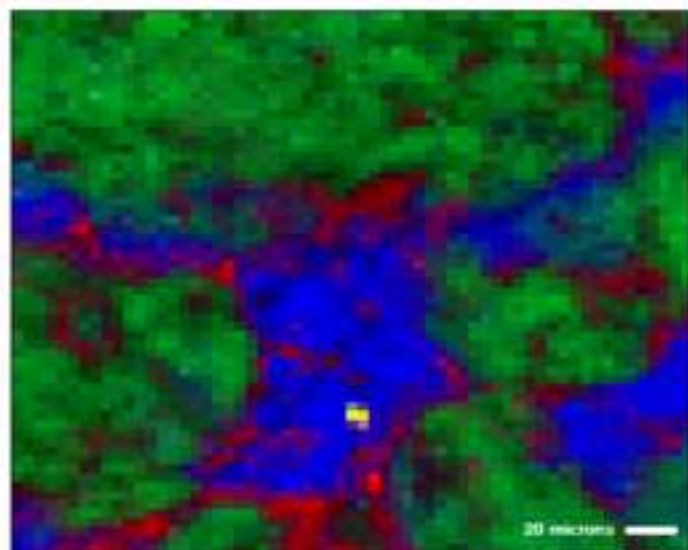








a)



b)

